Mater.Phys.Mech.1 (2000) 127-132

HIGH-STRENGTH NANOCRYSTALLINE Ni-W ALLOYS PRODUCED BY ELECTRODEPOSITION

Tohru Yamasaki

Department of Materials Science & Engineering, Faculty of Engineering, Himeji Institute of Technology, 2167 Shosha, Himeji, Hyogo 671-2201, Japan.

Received: June 7, 2000

Abstract. Nanocrystalline Ni-W alloys having both high ductility and high strength were produced by electrodeoisition. The plating bath for the electrodeposition contained nickel sulfate, citric acid, sodium tungstate and ammonium chloride, and was operated at various bath concentrations and conditions of electrolysis. The ductility and tensile strength of the deposited alloys are strongly influenced by inclusion of codeposited hydrogen during deposition process. After degassing the hydrogen, the high-strength nanocrystalline Ni-W alloy containing about 20.7 at. % W with an average grain size of about 3 nm has been obtained: the tensile strength attained to about 2300 MPa. The high ductility of this alloy was also observed: bending through an angle of 180 degree was possible without breaking.

1. INTRODUCTION

Nanocrystalline metallic materials are generally limited in practical applications because of their severe brittleness. It has not yet been well understood whether their brittle behavior is due to an intrinsic feature of nanocrystalline materials, or whether this is due to processing difficulties for the fine grain sizes such as an imperfect consolidation of the nanocrystalline powders [1]. On the other hand, electrodeposition is a superior technique for producing nanocrystalline materials having grain sizes anywhere from the essentially amorphous to nanoscaled materials for the grain sizes of about 5-50 nm in bulk form or as coatings with no post-processing requirements. However, most of the electrodeposited alloys have also exhibited the severe brittleness [2, 3].

In our previous study, we developed an aqueous plating bath for producing the amorphous and nanocrystalline Ni-W alloys having high hardness and good ductility [4-7]. They can be bent through an angle of 180 degree without breaking. The purpose of this presentation is to show that the nanocrystalline Ni-W alloys having high tensile strength of about 2300 MPa with good ductility can be produced by electrodeposition. In addition, embrittlement behaviors of the Ni-W electrodeposits during annealing has been studied, and a mechanism for the brittleness in nanocrystalline materials has been discussed.

2. EXPERIMENTAL PROCEDURE

The plating bath compositions and conditions selected for this study are shown in Table 1. Citric acid and ammonium chloride were introduced as complexing agents to form complexes with both Ni and W in the plating bath solution. To improve conductivity, sodium bromide was used. Electrodeposition was done on Cu sheets as substrates prepared by electropolishing, and a high purity platinum sheet was used as the anode. The plating cells, 600 ml beakers, each containing 500 ml of the bath were supported in a thermostat to maintain the desired bath temperature. A fresh plating bath was made for each experiment using analytical reagent grade chemicals and deionized water. The deposition rate of the Ni-W alloys was determined by weighting the substrate before and after the 1 h electrodeposition and calculating the additional mass per square centimeter. The electrodeposited Ni-W films were separated from the Cu substrates by immersing the samples in an aqueous solution containing CrO_3 (250 g/L) and H_2SO_4 (15 cc/L).

Structural analysis of the electrodeposited alloys was performed by means of X-ray diffraction using Cu-K_α radiation (Rotating anode type X-ray apparatus, Rigaku RINT-1500, 40 kV-200 mA) and high resolution electron microscopy (HRTEM, JEM-2010, 200kV). Elemental concentrations of the electrodeposits were analyzed by wavelength-crystal dispersion X-ray spec-

Corresponding author: Tohru Yamasaki, e-mail: yamasaki@mse.eng.himeji-tech.ac.jp

Table 1. Plating Bath Compositions and Conditions for Ni-W electrodeposition.

Nickel Sulfate,	$NiSO_4$-$6H_2O$	0.06 mol/L
Citric Acid,	$Na_3C_6H_5O_7$-$2H_2O$	0.5 mol/L
Sodium Tungstate,	Na_2WO_4-$2H_2O$	0.14 mol/L
Ammonium Chloride,	NH_4Cl	0.5 mol/L
Sodium Bromide,	NaBr	0.15 mol/L
Bath Temperature	348	K
pH	7.5	
Current Density	0.05~0.2	A/cm^2

troscopy (WDS) in a scanning electron microscope (JXA-8900R, 15 kV). The samples thus prepared were annealed at various temperatures. The degree of ductility was determined by measuring the radius of curvature at which the fracture occurred in a simple bending test. The fracture strain on the outer surface of the specimen, ε_f, is estimated by the equation, $\varepsilon_f = t/(2r\text{-}t)$, where r is the radius of curvature on the outer surface of the bend sample at fracture and t is the thickness of specimen. Vickers microhardness was measured by using the as-electrodeposited and the annealed samples on Cu substrates with a 0.02 kg load and a loading time of 15 s in cross section. The tensile test was carried out for the electrodeposited films having thickness of about 35 μm by using an Instron-type machine.

3. RESULTS

Structure of Ni-W electrodeposits. Structure of the Ni-W electrodeposits is strongly influenced by the plating bath conditions. Fig. 1 shows X-ray diffraction patterns of as-electrodeposited Ni-W alloys for various current densities between 0.05 and 0.2 A/cm^2 at a plating bath temperature of 348° K. X-ray diffraction peaks of the deposited alloys broadened and the tungsten content tended to increase with increasing applied current density. The amorphous pattern appeared at a tungsten content of more than about 20 at. %. Under these plating conditions, the Ni-W electrodeposits having amorphous and nanocrystalline structures were ductile: they could be bent through an angle of 180° without breaking (ε_f=1.0). Average grain sizes and Vickers microhardnesses of the as-electrodeposited Ni-W alloys for various current densities between 0.05 and 0.2 A/cm^2 are collected in Table 2. Average grain sizes in the Ni-W electrodeposits were obtained by applying the Scherrer formula to the diffraction lines of *fcc*-Ni (111) and the broad maximum of the amorphous phase, and also by direct observations from TEM micrographs. With increasing applied current density, the average grain size decreased and the Vickers microhardness increased continuously. On annealing these materials at 723 K for 24 h, grain growth occurred to 8.2~9.5 nm, and the hardness was largely increased to more than HV900. However, these annealed Ni-W electrodeposits exhibited the severe brittleness.

Fig. 2 shows a TEM images and the corresponding selected area diffraction pattern of the Ni-20.7 at. % W alloy electrodeposited with an applied current densities of 0.1 A/cm^2. As shown in this figure, grain sizes of the nanocrystalline structure ranged between 2.5 and 3.5 nm are observed. The selected area diffraction pattern consists only amorphous-like halos. Fig. 2 (b)

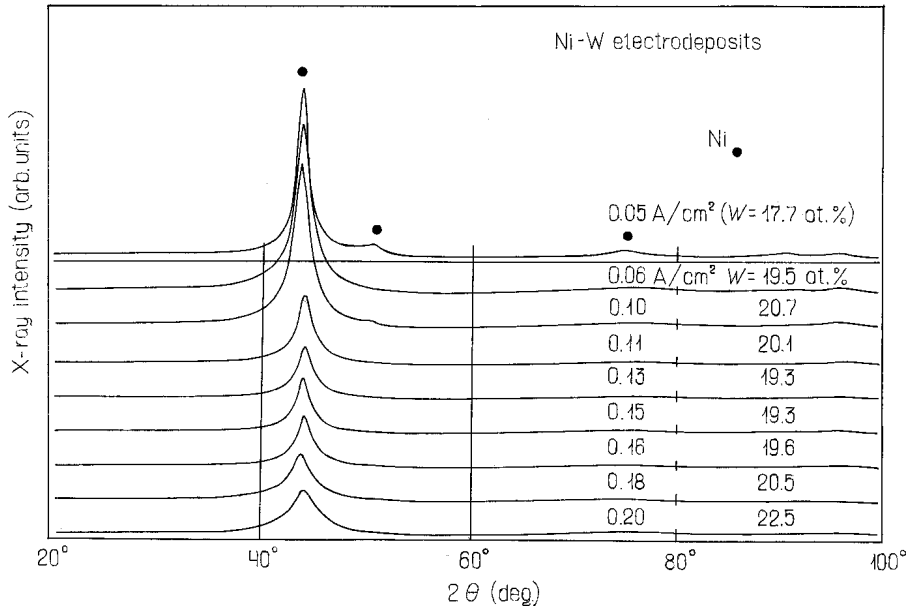

Fig. 1. X-ray diffraction patterns of as-electrodeposited Ni-W alloys for various current densities between 0.05 and 0.2 A/cm^2. All of these Ni-W alloys are ductile: they can be bent through an angle of 180 degree without breaking.

Table 2. Average grain sizes and Vickers microhardnesses of as-electrodeposited Ni-W alloys at a plating bath temperature of 348° K for various current densities and of annealed ones (723° K for 24 h in vacuum).

Current density (A/cm^2)	W content (at. %)	Grain size (nm), as-deposited	HV, as-deposited	Grain size (nm), 723K-24 h	HV, 723K-24 h
0.05	17.7	6.8 (7.0)*	558	9.5	919
0.10	20.7	4.7 (3.0)*	635	9.0 (10)*	962
0.15	19.3	4.7	678	8.9	992
0.20	22.5	2.5 (Am.)*	685	8.2	997

( )* : TEM observations

shows the high resolution *fcc*-(111) lattice image of this alloy having nanocrystalline structure with grain sizes between 2.5 and 3.5 nm. These grains are roughly spherical and do not have clear interface with the intercrystalline regions. In the intercrystalline regions that are about 1 to 2 nm in widths, distorted lattice images (i.e., the amorphous-like images) are observed. Similar features of HR-TEM observations have been observed in Ni-W alloys having grain sizes between 5 and 8 nm prepared by annealing the amorphous electrodeposited Ni-25.0 at. % W alloy [5].

Mechanical Properties of Nanocrystalline Ni-W electrodeposits. Fig. 3 shows stress-strain curves obtained by tensile tests for the electrodeposited Ni-20.7 at. % W alloys having grain size of about 3 nm. In order to clarify the effect of inclusion of codeposited hydrogen during deposition process, the curves for the degassed specimens at 353° K for 24 h in vacuum are also shown. The result varied considerably from specimen to specimen, being very sensitive to the residual hydrogen. In the case of the as-electrodeposited alloys, the tensile strength and the elongation at fracture were attained to 670 MPa and about ~0 %, respectively. After degassing at 353 K, the tensile strength and the elongation at fracture increased largely to 2333 MPa and about 0.5 %, respectively. Fig. 4 shows SEM images of fractured surfaces of tensile specimens of the as-electrodeposited and the degassed Ni-W alloys. Their fracture surfaces are fairly typical of ductile amorphous alloys. Typical river or vein patterns on the fracture surfaces are observed and demonstrate local plastic deformation.

4. DISCUSSION

Critical Grain Size for Keeping Good Ductility in Nanocrystalline Alloys. As shown in Table 2 and Fig. 3, nanocrystalline Ni-W alloys having grain sizes from

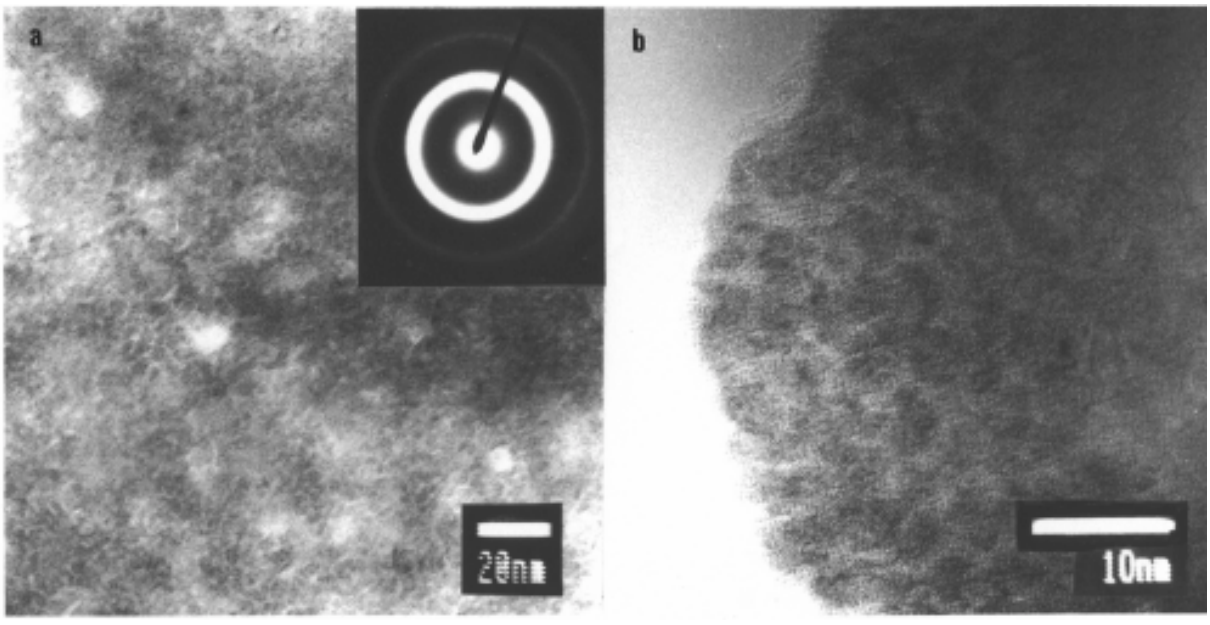

Fig. 2. TEM micrographs showing 2.5 ~ 3.5 nm particles and the selected area diffraction pattern in the as-electrodeposited Ni-20.7 at. % W alloy.

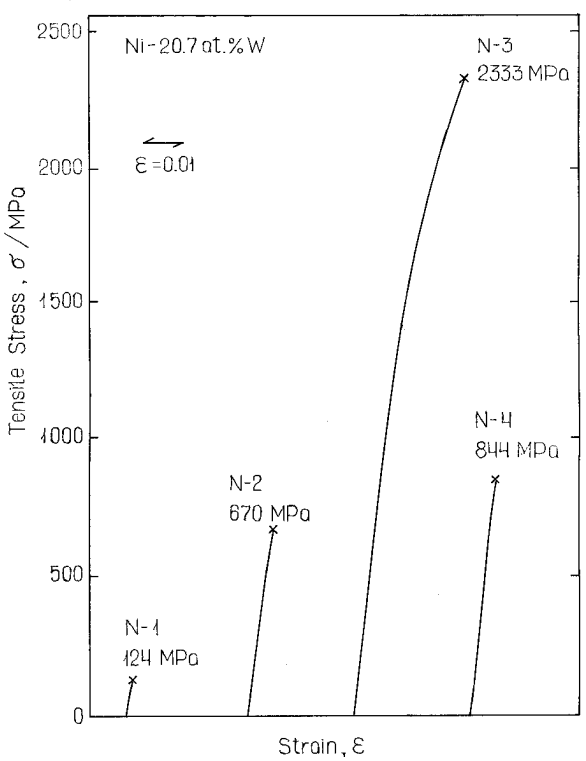

Fig. 3. Stress-strain curves obtained by tensile tests for the electrodeposited Ni-20.7 at. % W alloys having grain sizes of about 3 nm. The gage length, the thickness of the specimens and the strain rate are 15 mm, about 35 mm and 0.01/s, respectively. (N-1) & (N-2): as-electrodeposited specimens, (N-3) & (N-4): degassed specimens at 353 K for 24 h in vacuum.

the essentially amorphous to about 7 nm in diameter have exhibited the high hardness combined with the good ductility. Especially, the Ni-20.7 at. % W alloy having grain size of about 3 nm exhibited the high tensile strength of 2333 MPa. However, on annealing these materials at 723° K for 24 h, grain growth occurred to 8.2~9.5 nm, and they lost their ductility.

In order to estimate the critical grain size for keeping the good ductility in the nanocrystalline alloys, grain boundary sliding is considered to occur along suitable intercrystalline planes. Fig. 5 shows schematic explanations of the modeling of deformation by grain boundary sliding, with nanoscaled spherical hard grains being represented as a densely packed array of fcc crystal-type structure. As sliding occurs, close-packed planes of the nanoscaled grains do this easily than planes aligned in another direction. Thickness of these sliding planes (Δ) is derived from the following equation,

$$\Delta = (\frac{\sqrt{3}}{2} - 1)d + D, \qquad (1)$$

where d and D are the grain diameter and the grain boundary thickness, respectively. In this case, the grain diameter (d) is defined as the total length of the internal diameter of the grains and the grain boundary thickness. As shown in this figure, thickness of the sliding planes (Δ) decreases with increasing the grain size (d)

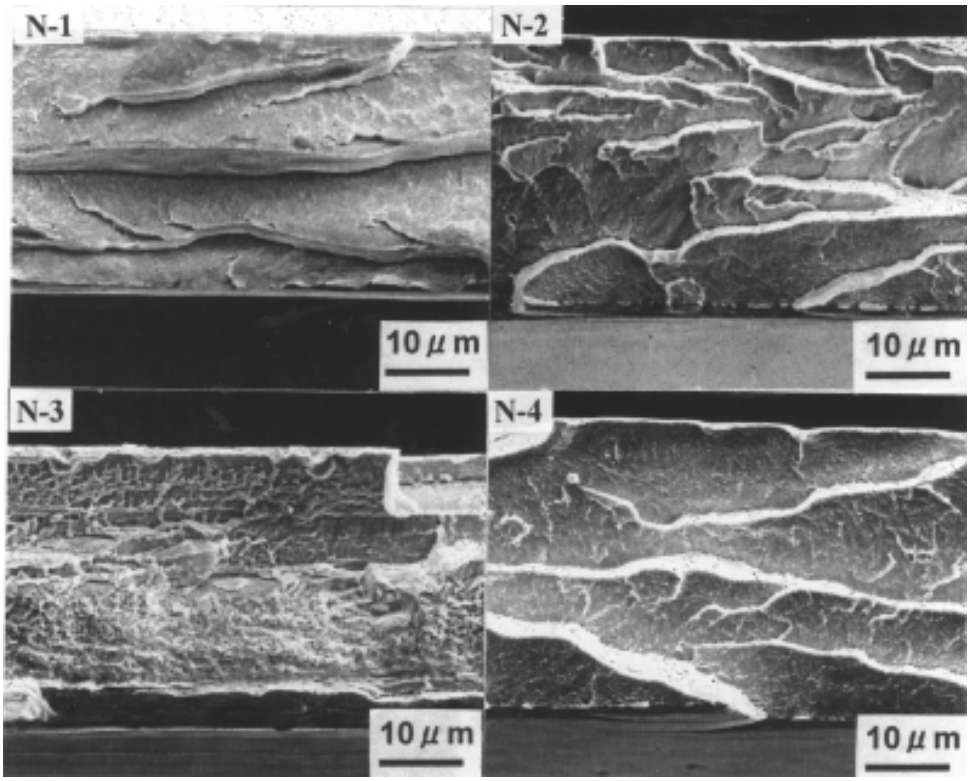

Fig. 4. SEM micrographs showing the fracture surfaces of the tensile specimens of the as-electrodeposited and the degassed Ni-20.7 at. % W alloys. (N-1) & (N-2): as-electrodeposited specimens, (N-3) & (N-4): degassed specimens at 353 K for 24 h in vacuum.

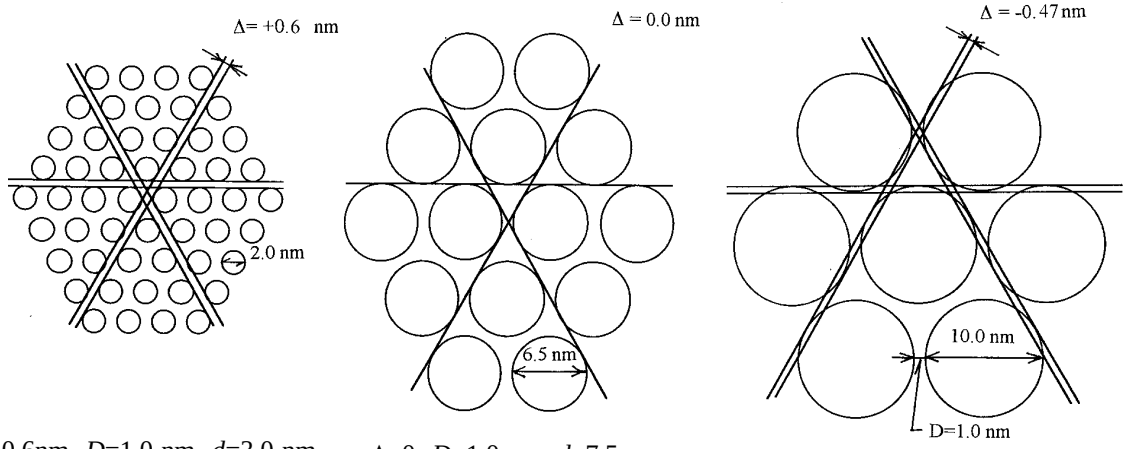

Δ=+0.6nm *D*=1.0 nm *d*=3.0 nm *d-D*=0.2 nm V_f^{ic}=70.4%

Δ=0 *D*=1.0 nm *d*=7.5 nm *d-D*=6.5 nm V_f^{ic}=34.9%

Δ=-0.47 nm *D*=1.0 nm *d*=11.0 nm *d-D*=10.0 nm V_f^{ic}=24.9%

Fig. 5. Schematic explanations of the modeling of deformation of nanocrystalline materials by grain boundary sliding. Grain boundary sliding is considered to occur along the close-packed planes of the nanocrystalline grains. The typical calculated values of *d*, *d-D*, Δ and V_f^{ic} have also shown in this figure under the condition of *D*=1.0 nm, where *d*, *D*, *d-D*, Δ and V_f^{ic} are the grain diameter, the grain boundary thickness, the internal grain diameter, the thickness of the planes for grain boundary sliding and the intercrystalline volume fractions, respectively.

under the condition where the grain boundary thickness (*D*) is constant, and then the Δ becomes zero and finally becomes negative. When the Δ is negative, grain boundary sliding becomes difficult and these materials should lost their ductility. We have defined the critical grain size (d_c) to keep the good ductility in nanocrystalline materials as the grain size under the condition where the Δ is zero.

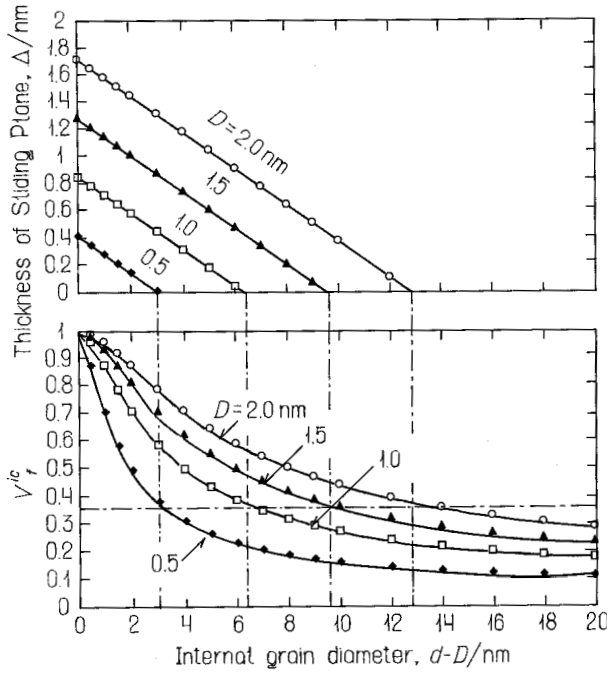

Fig. 6. Calcutlated thickness of the planes for the grain boundary sliding (Δ) and the intercrystalline volume fractions (V_f^{ic}) as a function of the internal diameter of the grains (*d-D*) where the grain boundary thickness (*D*) is changed over a range from 0.5 to 2.0 nm.

Fig. 6 shows the calculated Δ and intercrystalline volume fractions (V_f^{ic}) as a function of the internal diameter of the grains (*d - D*) where the *D* is changed over a range from 0.5 to 2.0 nm. The intercrystalline volume fraction is derived from the following equation,

$$V_f^{ic} = 1 - \left[(d - D) / d\right]^3 \quad (2)$$

As shown in this figure, the Δ decreases linearly with increasing the internal diameter of the grains (*d-D*). For example, when the *D* is taken as 1.5 nm, the (*d-D*) is about 9.7 nm under the condition of the Δ=0, and the critical grain size (d_c) can be obtained as 11.2 nm in diameter. Under the condition of Δ=0, the values of V_f^{ic} attained to the same values of about 35 % where the *D* is changed over a range from 0.5 to 2.0 nm.

Fig. 7 shows the fracture strain, ε_f, and the Vickers microhardness as a function of the grain size for the electrodeposited Ni-20.7 at. % W alloys. Average grain sizes were obtained by applying the Scherrer formula to the diffraction lines. The fracture strain decreased and the hardness increased with increasing the grain size. When the grain size increased to about 9 nm, they exhibited the severe brittleness and the hardness attained to a maximum value of about HV950. Assuming the grain size obtained by the X-ray diffraction is equal to the internal grain diameter (*d - D*), the critical grain size (d_c) can be estimated to about 10 ~ 11 nm in diameter for the grain boundary thickness of 1 to 2 nm as observed from the TEM micrographs. This data may be in good agreement with the critical value of d_c predicted from the Eq. 1 for the grain boundary thickness of 1.5 nm.

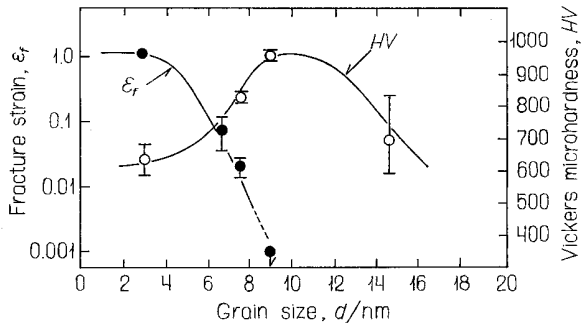

Fig. 7. The fracture strain (ε_f) obtained by simple bend tests and the Vickers microhardness as a function of grain size for the electrodeposited Ni-20.7 at. % W alloys.

It has been reported that some Al-based and Zr-based multicomponent amorphous alloys containing finely dispersed nanoscaled crystallites exhibit high fracture strength and high ductility. In the Al-based alloys, they exhibit their good ductility when the volume fraction of the crystallites (V_{fc}) is less than about 30 % (i.e., V_f^{ic} > 70%) [8,9]. In the case of the melt-spum Zr-Al-Cu-Pd alloys, however, fracture strength increased linearly with increasing the V_{fc} up to about V_{fc}=75% (i.e., V_f^{ic} = 25%) [10]. Suitable volume fraction of the crystallites to keep the high-strength in the nanocrystalline materials should be depend on the deformability of the intercrystalline regions. But, our proposed sliding model could apply to estimate the ductile/brittle behaviors of nanocrystalline materials. The effects of the deformability of the intercrystalline regions on the critical grain size (d_c) are matters of future research.

5. CONCLUSIONS

The nanocrystalline Ni-W electrodeposited alloys having high tensile strength and good ductility with completely bending (ε_f=1.0) were obtained. Especially, the high-strength nanocrystalline Ni-W alloy containing about 20.7 at. % W with an average grain size of about 3 nm has been obtained: the tensile strength was attained to 2333 MPa combined with the good ductility. On annealing these materials at various temperatures, however, grain growth occurred and they lost their ductility. In order to estimate the critical grain size for keeping the good ductility in the nanocrystalline alloys, grain boundary sliding is considered to occur along the close-packed planes of the nanocrystalline grains under the condition where the nanoscaled spherical hard grains is represented as a densely packed array.

ACKNOWLEDGMENTS

This work was supported by a Grant-in-Aid for Scientific Research from the Ministry of Education, Science, Sports and Culture, Japan. The author is deeply grateful to Miss R. Tomohira and Mr. S. Yamashita in Himeji Institute of Technology for their experimental assistance.

REFERENCES

[1] D. G. Morris, *Mechanical Behaviour of Nanostructured Materials, Materials Science Fundations 2*, (Trans Tech Publications, 1998).
[2] A. M. El-Sherik and U. Erb // *Plating & Surface Finishing* **82** (1995) 85.
[3] K. Suzuki, F. Itoh, T. Fukunaga and T. Honda, *Proc. of 3rd Int. Conf. of Rapidly Quenched Metals* (Brighton, Vol. **2,** 1978) 410.
[4] W. Ehrfeld, V. Hessel, H. Loewe, Ch. Schulz and L. Weber, *Proc. of 2nd Int. Conf. of Micro Materials "97* (Berlin, 1997) 112.
[5] T. Yamasaki, P. Schlossmacher, K. Ehrlich and Y. Ogino // *NanoStructured Materials* **10** (1998) 375.
[6] T. Yamasaki, R. Tomohira and Y. Ogino, In: *Proc. of Int. Conf. on Solid-Solid Phase Transformations*, ed. by M. Koiwa et al., Vol. **2** (The Japan Institute of Metals, 1999), 1247.
[7] T. Yamasaki, R. Tomohira, Y. Ogino, P. Schlossmacher and K. Ehrlich // *Plating & Surface Finishing* **87** (2000) 148.
[8] Y.-H. Kim, A. Inoue and T. Masumoto // *Materials Trans., JIM* **31** (1990) 747.
[9] H. Chen, Y. He, G. J. Shiflet and S. J. Poon // *Scripta Metallurgica et Materialia* **25** (1991) 1421.
[10] A. Ionue, C. Fan and T. Zhang, In: *Proc. of Int. Conf. on Solid-Solid Phase Transformations*, ed. by M. Koiwa et al., Vol. **2** (The Japan Institute of Metals, 1999), 1199.